A&A 492, 111–115 (2008)
DOI: 10.1051/0004-6361:200810942

Astronomy & Astrophysics

On the central ionizing star of G23.96+0.15 and near-IR spectral classification of O stars *(Research Note)*

P. A. Crowther and J. P. Furness⋆

Department of Physics & Astronomy, University of Sheffield, Hounsfield Road, Sheffield, S3 7RH, UK
e-mail: Paul.Crowther@sheffield.ac.uk

Received 9 September 2008 / Accepted 14 October 2008

ABSTRACT

Aims. A near-infrared study of the main ionizing star of the ultracompact HII region G23.96+0.15 (IRAS 18317–0757) is presented, along with a re-evaluation of the distance to this source, and a re-assessment of *H*- and *K*-band classification diagnostics for O dwarfs
Methods. We have obtained near-IR VLT/ISAAC imaging and spectroscopy of G23.96+0.15, plus archival imaging from UKIRT/UFTI. A spectroscopic analysis was carried out using a non-LTE model atmosphere code.
Results. A quantitative *H*- and *K*-band classification scheme for O dwarfs is provided, from which we establish an O7.5V spectral subtype for the central star of G23.96+0.15. We estimate an effective temperature of $T_{\rm eff} \sim 38$ kK from a spectral analysis.
Conclusions. A spectroscopic distance of 2.5 kpc is obtained for G23.96+0.15, substantially lower than the kinematic distance of 4.7 kpc, in common with recent studies of other Milky way H II regions. Such discrepancies would be alleviated if sources are unresolved binaries or clusters.

Key words. ISM: HII regions – ISM: dust, extinction – stars: early-type – stars: fundamental parameters

1. Introduction

The formation of high mass stars remains an unresolved problem in contemporary astrophysics (Zinnecker & Yorke 2007). Despite considerable theoretical progress in recent years, this topic remains observationally challenging. O stars form deeply embedded within their natal cocoons, presumably within intermediate to high mass star clusters, only to visually emerge after ~0.5 Myr (Prescott et al. 2007), a substantial fraction of their 2–10 Myr main-sequence lifetimes.

Radio continuum surveys of ultracompact H II (UCHII) regions betray the presence of O stars through the effect of their Lyman continuum photons to free-free (thermal) emission. Typically, these regions can not be observed at wavelengths shorter than the mid-infrared, such that the ionizing stars can only be studied indirectly through the circumstellar dust and gas (e.g. Peeters et al. 2002; Martín-Hernández et al. 2002). However, in a few instances our sight line to the central source is sufficiently clear of circumstellar dust that the O star responsible for the H II region can be directly observed at near-infrared wavelengths (Watson & Hanson 1997; Hanson et al. 2002; Bik et al. 2005).

Over the past decade, the advent of efficient near-IR spectrographs at large ground-based telescopes has permitted medium resolution ($R \sim 5000$) spectroscopy of template Milky Way O stars in the *H*- and *K*-bands (Hanson et al. 2005b), which has been extended to the O4–5 star responsible for the G29.96–0.02 UCHII region (IRAS 8434–0242, Hanson et al. 2005a). Spectroscopic analysis of near-IR hydrogen and helium lines of O stars agrees closely with optical diagnostics in most cases (Repolust et al. 2005).

Thus far, G29.96–0.02 represents the sole example of an UCHII region whose ionizing star has been analysed based upon medium spectral resolution. The significance of such objects is that, in principal, they may serve as calibrators for the so-called "inverse problem", in which the ionizing stars of embedded UCHII regions may be obtained from analysis of mid-infrared fine-structure nebular lines (e.g. Martín-Hernández et al. 2002; Morisset et al. 2004).

Fortunately, other UCHII regions are also accessible to near-IR spectroscopy. One such region, G23.96+0.15 (IRAS 18317–0757) is the focus of the present study, for which Hanson et al. (2002) estimated a spectral type of O7–8 from low resolution *K*-band spectroscopy and Kim & Koo (2001) have inferred a mid-O spectral type from radio continuum observations for an adopted distance of 6 kpc. Hunter et al. (2004) have identified a cluster of embedded massive stars from millimetre observations of G23.96+0.15.

In the present study, we present new near-IR imaging and spectroscopy of G23.96+0.15 permitting the subtype of the ionizing star to be refined from *H*-band and *K*-band hydrogen and helium line ratios, plus a spectroscopic distance for comparison with kinematic results.

2. Observations

H-band and *K*-band spectroscopy of G23.96+0.15 was observed with the ISAAC instrument (Moorwood et al. 1998) mounted at the Very Large Telescope between 22 April-2 May 2006. High spatial resolution imaging was drawn from acquisition ISAAC datasets, which were supplemented by archival UKIRT Fast

⋆ Based on observations made with ESO telescopes at the Paranal Observatory under programme ID 077.C-0550(A).

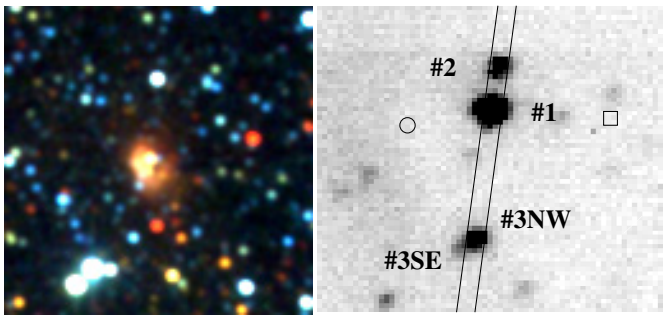

Fig. 1. (*left*) 2 × 2 arcmin composite *JHK* image centered upon G23.96+0.15 from 2MASS; (*right*) 10 × 10 arcsec ~2.18 μm acquisition image of G23.96+0.15 from ISAAC, in which the brightest sources are marked with the ISAAC slit overlaid. Source #1 has position α = 18:34:25.25, δ = –07:54:45.5 (J2000), with the locations of the 6 cm peak from Wood & Churchwell (1989, circle) and 21 cm peak from Kim & Koo (2001, square) also indicated. North is up and east is to the left. (This figure is available in color in this electronic version.)

Trace Imager (UFTI, Roche et al. 2002) *K*-band imaging, plus *H*-band imaging from Hanson et al. (2002) and 2MASS datasets.

2.1. Near-IR imaging

Acquisition ISAAC images of G23.96+0.15 were obtained using the 1024 × 1024 Hawaii Rockwell array (0.148 arcsec/pix), with a combination of both the 2.17 μm and 2.19 μm narrow-band filters during excellent seeing conditions of 0.3–0.5 arcsec in April–May 2006.

In Fig. 1 we present a 2 × 2 arcmin *JHK* composite image centered upon G23.96+0.15 from 2MASS plus the central 10 × 10 arcsec of the ~2.18 μm ISAAC dataset. The ISAAC image reveals a bright source (#1), located at α = 18:34:25.25, δ = −07:54:45.5 (J2000.0). This source lies ~2.7 arcsec west of the 6 cm peak reported by Wood & Churchwell (1989), though 3.5 arcsec east of the 21 cm peak of Kim & Koo (2001) for this irregular UCHII region. Fainter near-IR sources lie 1.5 arcsec to the north of #1 and 4.2 arcsec to the south, which we shall refer to as sources #2 and 3, respectively. Source #3 is itself resolved into NW and SE components, separated by 0.7 arcsec. Photometry of these sources was obtained from archival UKIRT UFTI images from 19 Jul. 2000 obtained with the 1024 × 1024 Hawaii array (0.09 arcsec/pix) and *K*-band (K98) filter during seeing conditions of ~0.6 arcsec, using a zero-point obtained from 10 nearby 2MASS field stars, providing an accuracy of ±0.04 mag. The *J*-, *H*- and *K*-band magnitudes for the combined sources #1 and #2 are 13.81, 11.46 and 9.94 mag, respectively (2MASS 18342523-0754455).

We have also inspected *H*-band images from the Steward 2.3 m IRCam guider images of Hanson et al. (2002) using a 128 × 128 Hawaii array (0.5 arcsec/pix), obtained in seeing conditions of ~1.5 arcsec, in which sources #1 and #2 are again blended, from which H(#3) – H(#1 + #2) ~1.5 mag. Independent estimates of H(#3NW) – H(#2) ~0.3 mag and H(#3NW) – H(#1) ~2.3 mag have been obtained from our high spatial resolution ISAAC 1.71 μm long-slit spectroscopy (see next section). These sources were well aligned, so slit losses should minimal. Photometric properties are presented in Table 1, taking into account uncertainties resulting from the ISAAC and IRCam observations.

Table 1. Near-IR properties of G23.96+0.15 sources from UKIRT/UFTI (*K*-band) and Steward 2.3 m/IRCam imaging (*H*-band) plus VLT/ISAAC acquisition images and spectroscopy, from which equivalenth widths (W_λ in Å) were also measured for #1.

Source	K Mag	$H-K$ Mag	W_λ(He II) 1.692 μm	W_λ(He I) 1.700 μm	W_λ(H I) 2.165 μm	W_λ(He II) 2.189 μm	Spect. Type
#1	10.43	1.2	0.20	1.24	2.95	0.94	O7.5V
	±0.04	±0.1	±0.08	±0.11	±0.17	±0.12	
#2	12.00	1.7					
	±0.04	±0.2					
#3NW	12.10	1.9					
	±0.04	±0.3					
#3SE	13.7	–0.2					
	±0.2	±0.3					

2.2. Near-IR spectroscopy

Long-slit spectroscopy of G23.96+0.15 was obtained with ISAAC in April–May 2006 at a position angle of 7.7 degrees west of north, in order to include sources #1, #2 and #3NW at three medium resolution, 0.775 Å/pix) grating settings centered at 1.71, 2.09 and 2.20 μm (recall Fig. 1). These observations, obtained using a 0.6 arcsec slit width, were taken during excellent seeing conditions (0.3–0.5 arcsec) at low airmass (1.02–1.08) together with solar-type telluric analogues.

Six individual exposures, comprising three AB pairs, were obtained for each grating setting, with wavelength solutions achieved from comparison XeAr arc datasets. From these, the observations covered 1.671–1.751 μm, 2.029–2.155 μm and 2.140–2.265 μm at spectral resolutions of 3.8 Å, 6.0 Å and 6.0 Å respectively, as measured from arc lines.

Telluric correction was achieved from a single AB pair of spectroscopic datasets of early-G dwarfs observed at a similar airmass to G23.96+0.15, corrected for their spectral features using high resolution observations of the Sun which were adjusted to both the radial velocity and spectral resolution of the template stars.

The 2.09 μm setup suffered from low-level variable structure which was accentuated upon flat-fielding, so that only the two other settings were flat-fielded. Consequently, the continuum S/N achieved was ~100 for the 1.71 μm setting and 150 for the 2.20 μm setting for #1, but only 60 for the 2.09 μm setting. The continuum S/N for sources #2 and #3NW was, at best, no greater than 40–50.

3. The ionizing star of G23.96+0.15

3.1. Near-IR spectral classification

Hanson et al. (1996) developed a classification scheme for O stars from low resolution *K*-band spectroscopy. Classification of early to mid-O stars was achieved from the presence of C IV 2.08 μm and N III 2.11 μm emission lines, although it proved to be problematic to distinguish between late O and early B stars. This technique was extended to the *H*-band by Hanson et al. (1998) who highlighted the diagnostic role of the hydrogen Br 11 1.681 μm, He II 1.692 μm and He I 1.700 μm lines.

In Fig. 2 we present *H*-band and *K*-band spectroscopy of G23.96+0.15 #1 together with MK classification O dwarfs from the high quality, medium resolution atlas of Hanson et al. (2005b). From visual inspection, a classification of O7–8 is estimated, in agreement with the low resolution *K*-band spectrum of #1 from Hanson et al. (2002). However, we have also investigated the possibility of using the He II 1.692 μm/He I 1.700 μm

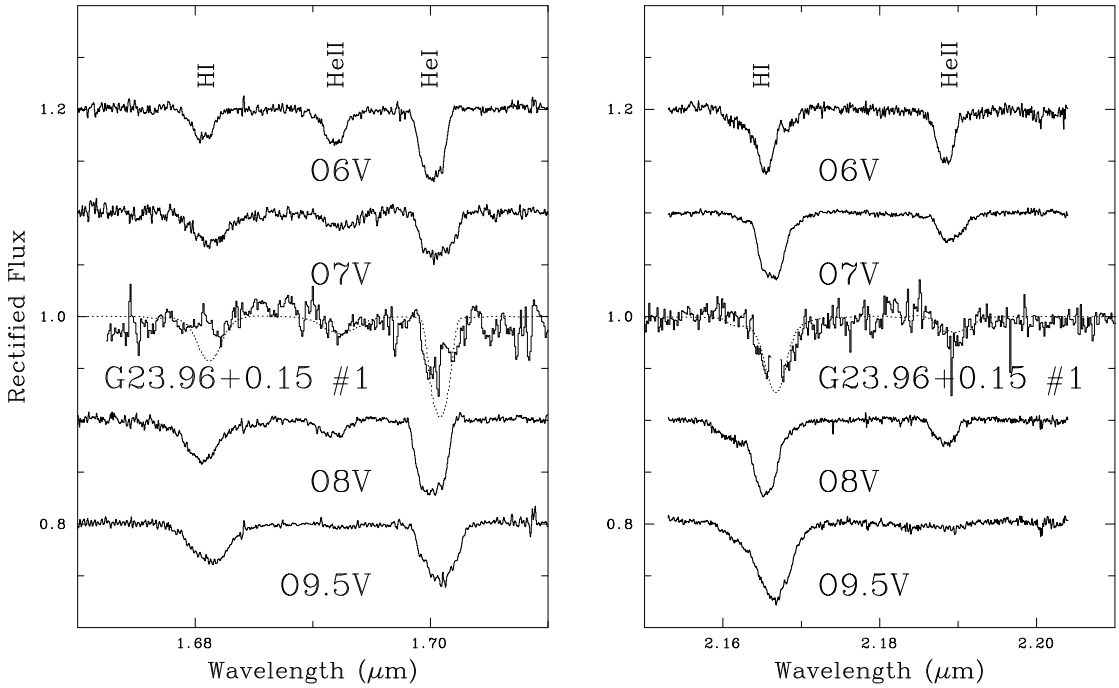

Fig. 2. *H*-band (*left*) and *K*-band (*right*) VLT/ISAAC spectroscopy of G23.96+0.15 #1 together with MK template O6–9.5V stars from Hanson et al. (2005b), together with a spectral fit to #1 (dotted line, see text).

and He II 2.189 μm/Brγ ratios for quantitative classification, independent of the metal lines in the *K*-band (see also Lenorzer et al. 2004; Repolust et al. 2005).

We have measured the equivalent widths of these lines for MK classification O stars from Hanson et al. (2005b), whose absorption line ratios are presented in Fig. 3 (excluding Brγ emission line supergiants). From this it is clear that the He II 1.692 μm/He I 1.700 μm ratio provides an excellent classification diagnostic for O stars, especially dwarfs, while the He II 2.189 μm/Brγ ratio provides an additional constraint for late-type O dwarfs, providing the spectral resolution is sufficient to exclude any nebular contamination. Polynomial fits to equivalent width ratios of dwarf stars from Hanson et al. (2005b) are presented as a guide, excluding HD 37 468 from the fit for which negligible He II absorption is observed. The *H*-band ratio inherently represents a superior diagnostic, although the *K*-band ratio has two advantages for late-type O dwarfs, namely a lower interstellar extinction plus 2.189 μm is an intrinsically stronger He II line than 1.692 μm.

Unfortunately, the moderate S/N of sources #2 and #3 prevented identification of spectral feaures beyond Brγ nebular emission. We present *H* and *K*-band photometry of these sources in Table 1 together with absorption line measurements of G23.96+0.15 #1. From the lower S/N *H*-band ratio we infer a dwarf spectral type of $O8^{+1}_{-0.5}$ while the *K*-band diagnostic indicates O7.5 ± 0.5. Therefore, we propose an O7.5V classification for source #1.

3.2. Stellar temperature of G23.96+0.15 #1

The current spectroscopic calibration of O stars would result in an effective temperature of $T_{\rm eff}$ = 36 kK for an O7.5 star (Martins et al. 2005). Instead, we have obtained a direct estimate of the stellar temperature from a comparison between the near-IR hydrogen and helium lines and synthetic spectra obtained with the CMFGEN model atmosphere code (Hillier & Miller 1998).

CMFGEN solves the radiative transfer equation in the comoving frame, under the additional constraint of statistical equilibrium. The temperature structure is determined by radiative equilibrium. Since CMFGEN does not solve the momentum equation, a density or velocity structure is required. For the supersonic part, the velocity is parameterized with a classical β-type law, with an exponent of $\beta = 1$ adopted. This is connected to a hydrostatic density structure at depth, such that the velocity and velocity gradient match at the interface. The subsonic velocity structure is set by a corresponding fully line-blanketed plane-parallel TLUSTY model (v.200, see Lanz & Hubeny 2003). The atomic model is similar to that adopted in Hillier et al. (2003), including ions from H, He, C, N, O, Ne, Si, S, Ar, Ca and Fe.

We have assumed a depth-independent Doppler profile for all lines when solving for the atmospheric structure in the comoving frame, while in the final calculation of the emergent spectrum in the observer's frame, we have adopted a uniform turbulence of 50 km s^{-1}. Incoherent electron scattering and Stark broadening for hydrogen and helium lines are adopted. Finally, we convolve our synthetic spectrum with a rotational broadening profile.

For an adopted terminal wind velocity of 2000 km s^{-1}, surface gravity of $\log g = 4$ and abundance ratio of He/H = 0.1 by number, we varied the stellar radius and (non-clumped) mass-loss rate until a reasonable match to the He II 1.692 μm, He I 1.700 μm, Brγ and He II 2.189 μm was achieved. An acceptable fit was achieved for $T_{\rm eff}$ = 38 ± 1 kK, $\log \dot{M}/(M_\odot\,{\rm yr}^{-1})$ = −6.3 ± 0.2 and $v \sin i \sim 220 \pm 30$ km s^{-1}, as shown in Fig. 2. Nebular contamination is significant for He I 1.700 μm and high members of the hydrogen Brackett series. For an adopted mass of 30 $M_\odot$, a radius of 9.2 $R_\odot$ results, which is representative of normal Milky Way mid-O dwarfs (e.g. Repolust et al. 2005). We defer any further discussion of the physical properties of

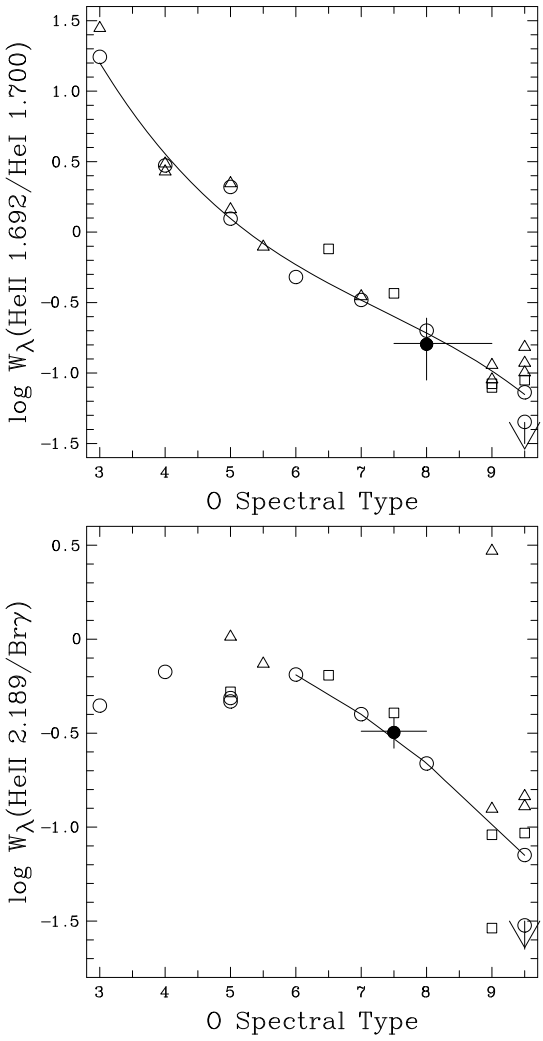

Fig. 3. (*Top*) Equivalent width ratio of He II 1.692 μm/He I 1.700 μm versus subtype for O dwarfs (circles), giants (squares) and supergiants (triangles) from Hanson et al. (2005a) and G23.96+0.15 #1 (filled circle) together with a polynomial fit to dwarfs as a guide (solid line); (*bottom*) as above for ratio of He II 2.189 μm/Brγ.

G23.96+0.15 #1 until the next section where its distance is considered.

4. Distance and extinction to G23.96+0.15

Distances to Galactic H II regions are typically obtained from kinematic methods, using an adopted rotation curve (Brand & Blitz 1993) and Solar galactocentric distance (8 kpc, Reid 1993). Following this approach the near (far) kinematic distance to G23.96+0.15 is 4.7 kpc (10.0 kpc) based upon the LSR velocity of 79.3 km s^{-1} from Wink et al. (1983), suggesting a distance of 4.2 kpc from the Galactic Centre for G23.96+0.15. LSR velocities from NH_3 (Churchwell et al. 1990), CS (Plume et al. 1992) and H76α recombination lines observations (Kim & Koo 2001) agree with Wink et al. (1983) to within $\pm$1 km s^{-1}.

One would expect $M_K = -3.9$ mag for G23.96+0.15 #1 (O7.5V) from the Conti et al. (2008) absolute visual magnitude-spectral type calibration, together with the intrinsic colours of Martins & Plez (2006). We may correct its observed K-band magnitude for extinction using $A_K = 1.82^{+0.30}_{-0.23} E_{H-K}$ (Indebetouw et al. 2005) and $(H-K)_0 = -0.10$ mag, from

Table 2. Physical properties of G23.96+0.15 #1 from our spectral analysis, based upon either the spectroscopic (*top*) or kinematic (*bottom*) distances. Mass estimates are approximate since we adopt $\log g = 4.0$. The predicted Lyman continuum ionizing flux (Q_0) is shown together with lower limits obtained from the 21 cm radio observations of Kim & Koo (2001, $Q_0^{\rm KK01}$).

$T_{\rm eff}$ kK	$\log L$ $L_\odot$	M $M_\odot$	$\log \dot{M}$ $M_\odot$ yr^{-1}	$\log Q_0$ s^{-1}	$\log Q_0^{\rm KK01}$ s^{-1}	M_K mag	d kpc
38	5.2	30	−6.3	48.8	≥48.1	−3.9	2.5
38	5.8	130	−5.8	49.4	≥48.6	−5.5	4.7

which $A_K = 2.33 \pm 0.3$ mag, suggesting a distance modulus of $12.0^{+0.3}_{-0.4}$, i.e. a distance of 2.5 ± 0.4 kpc. For a representative scatter of $\pm$0.5 mag in the absolute magnitude calibration of O stars, a spectroscopic distance in the range 2–3.2 kpc would be implied, placing G23.96+0.15 at a distance of 5.8 $\pm$ 0.5 kpc from the Galactic Centre.

Martín-Hernández et al. (2002) have previously estimated $A_K = 2.0$ mag for G23.96+0.15 based upon HI recombination lines observed in Infrared Space Observatory (ISO) spectroscopy. We independently confirm this result from the observed ISO Brα/Brβ ratio, although the ISO pointing was offset by ≥10 arcsec from the source peak, and so measured fluxes need to be treated with caution (Peeters et al. 2002).

In common with other studies of H II regions, we find a spectroscopic distance to G23.96+0.15 that is substantially lower than kinematic distances (e.g. Blum et al. 2001; Figueredo et al. 2008). The two distances could be reconciled if #1 were substantially more luminous than typical mid-O stars, with $M_K = -5.5$ mag, although this would require the star to be extremely massive if it is single. This is highlighted in Table 2, where physical properties of G23.96+0.15 #1 for each of the alternate distances are presented. Of course, #1 could be an unresolved equal mass binary (or compact star cluster). Such a source would appear ~0.75 (0.3) mag brighter in the K-band than a single O7.5 star, owing to the contribution of its companion(s)[1]. A binary/cluster scenario would help to alleviate the spectroscopic and kinematic distance discrepancy, although in the cluster case, stellar absorption lines from the O star would be diluted by the continuum light from lower mass cluster members, which does not appear to be the case for G23.96+0.15 #1 (recall Fig. 2). Similar remarks apply for G29.96–0.02, for which a spectroscopic distance of ~3 kpc would be expected for a single O4 dwarf using near-IR photometry from Pratap et al. (1999), compared with a kinematic distance of 7.4 kpc (Fish et al. 2003).

Kim & Koo (2001) estimated an ionizing output of $10^{48.8}$ ph s^{-1} for G23.96+0.15A from their 21 cm radio continuum observations, which is equivalent to an O7 dwarf (Conti et al. 2008), albeit based upon an assumed distance of 6 kpc. If one was to adjust the distance to 4.7 (2.5) kpc, a reduced Lyman continuum output would be obtained, representative of an O8 (O9.5) star (Table 2). The measured 21 cm flux, ~0.75 dex lower than our indirect estimate, is merely a lower limit since it may be partially optically thick to bremstrahlung radiation and a fraction of the ionizing photons are likely to be absorbed by dust (either within the H II region or circumstellar cocoon).

The near-IR colours of sources #2 and #3NW are consistent with being physically associated with G23.96+0.15 #1 (#3SE is likely a foreground source). For the spectroscopic distance of 2.5 kpc, they are probable early B dwarfs, at projected

[1] On the basis of a Salpeter-like Initial Mass Function for high mass stars.

distances of 0.02 pc (#2) and 0.05 pc (#3NW) from #1. In common with indirect dust and gas diagnostics for other UCHII regions (Okamoto et al. 2003), we find evidence that G23.96+0.15 likely hosts multiple massive stars (see also Hunter et al. 2004). For the kinematic (near) distance of 4.7 kpc, sources #2 and #3NW would possess absolute magnitudes typical of late O stars, and so would also most likely be unresolved sub-clusters within the UCHII region, at projected distances of 0.035–0.1 pc from #1.

5. Conclusions

We show that G23.96+0.15 provides a second UCHII region whose ionizing star (#1) is accessible to high S/N, medium resolution near-IR spectroscopy, complementing the higher ionization G29.96–0.02 source. We provide a quantitative near-infrared classification scheme for O stars, which has potential application for other visibly obscured O dwarfs in the Milky Way, from which a near-IR O7.5V classification is obtained for G23.96+0.15 #1. We obtain a stellar temperature of $T_{\rm eff}$ = 38 kK for G23.96+0.15 #1 and infer a spectroscopic distance of 2.5 kpc for a single star origin. This is substantially smaller than the (near) kinematic distance of 4.7 kpc, in common with other obscured H II regions (e.g. Blum et al. 2001; Figueredo et al. 2008), although an unresolved binary or cluster nature would help to alleviate this discrepancy. Two fainter sources are also likely early-type members of the UCHII region. The availability of spectral properties for G23.96+0.15 should help empirically address the "inverse problem" of obtaining the ionizing O stars for other UCHII regions based solely upon mid-IR nebular characteristics.

Acknowledgements. Many thanks to Margaret Hanson for providing her *H*-band image of G23.96+0.15 and intermediate resolution near-infrared spectral atlas. This publication makes use of data products from 2MASS, which is a joint project of the University of Massachusetts and the IPAC/CalTech, funded by the NASA and the NSF, and is, in part, based upon archival observations from UKIRT which is operated by the Joint Astronomy Centre on behalf of the Science and Technology Facilities Council (STFC) of the UK. J.P.F. acknowledges financial support from the STFC.

References

Bik, A., Kaper, L., Hanson, M. M., & Smits, M. 2005, A&A, 440, 121
Blum, R. D., Damineli, A., & Conti, P. S. 2001, AJ, 121, 3149
Brand, J., & Blitz, L. 1993, A&A, 275, 67
Churchwell, E., Walmsley, C. M., & Cesaroni, R. 1990, A&AS, 83, 119
Conti, P. S., Crowther, P. A., & Leitherer, C. 2008, From Luminous Hot Stars to Starburst Galaxies, Cambridge Astrophysics Series, 45 (Cambridge: CUP)
Figueredo, E., Blum, R. D., Damineli, A., Conti, P. S., & Barbosa, C. L. 2008, AJ, 136, 221
Fish, V. L., Reid, M. J., Wilner, D. J., & Churchwell, E. 2003, ApJ, 587, 701
Hanson, M. M., Conti, P. S., & Rieke, M. J. 1996, ApJS, 107, 281
Hanson, M. M., Rieke, G. H., & Luhman, K. L. 1998, AJ, 116, 1915
Hanson, M. M., Luhman, K. L., & Rieke, G. H. 2002, ApJS, 138, 35
Hanson, M. M., Puls, J., & Repolust, T. 2005a, in Proc. IAU Symp. 227, Massive Star Birth: a crossroads of astrophysics ed. R. Cesaroni, M. Felli, E. Churchwell, & M. Walmsley (Cambridge: CUP), 376
Hanson, M. M., Kudritzki, R.-P., Kenworthy, M. A., Puls, J., & Tokunaga, A. T. 2005b, ApJS, 161, 154
Hillier, D. J., & Miller, D. L. 1998, ApJ, 496, 407
Hillier, D. J., Lanz, T., Heap, S. R., et al. 2003, ApJ, 588, 1039
Hunter, T. R., Zhang, Q., & Sridharan, T. K. 2004, ApJ, 606, 929
Indebetouw, R., Mathis, J. S., Babler, B. L., et al. 2005, ApJ, 619, 931
Kim, K.-T., & Koo, B.-C. 2001, ApJ, 549, 979
Lenorzer, A., Mokiem, M. R., de Koter, A., & Puls, J. 2004, A&A, 422, 275
Martín-Hernández, N. L., Peeters, E., Morisset, C., et al. 2002, A&A, 381, 606
Martins, F., & Plez, B. 2006, A&A, 457, 637
Martins, F., Schaerer, D., & Hillier, D. J. 2005, A&A, 436, 1049
Moorwood, A., Cuby, J.-G., Biereichel, P., et al. 1998, ESO Messenger, 94, 7
Morriset, C., Schaerer, D., Bouret, J.-C., & Martins, F. 2004, A&A, 415, 577
Okamoto, Y. K., Kataza, H., Yamashita, T., et al. 2003, ApJ, 584, 368
Peeters, E., Martín-Hernández, N. L., Damour, F., et al. 2002, A&A, 381, 571
Plume, R., Jaffe, D. T., & Evans, N. J. 1992, ApJS, 78, 505
Pratap, P., Megeath, S. T., & Bergin, E. A. 1999, ApJ, 517, 799
Prescott, M. K. M., Kennicutt, R. C. Jr., Bendo, G. J., et al. 2007, ApJ, 668, 182
Reid, M. J. 1993, ARA&A, 31, 345
Repolust, T., Puls, J., Hanson, M. M., et al. 2005, A&A, 440, 261
Roche, R. F., et al. 2002, Proc. SPIE, 4841
Watson, A. M., & Hanson, M. M. 1997, ApJ, 490, L165
Wink, J. E., Wilson, T. L., & Bieging, J. H. 1983, A&A, 127, 211
Wood, D. O. S., & Churchwell, E. 1989, ApJS, 69, 831
Zinnecker, H., & Yorke, H. W. 2007, ARA&A, 45, 481